Penetration of ultraviolet radiation in the waters of the estuary and Gulf of St. Lawrence

Abstract—Downwelling ultraviolet (UV) irradiance (290–400) nm was measured at 1-nm intervals in the surface waters of the estuary and Gulf of St. Lawrence, Canada, in September 1996 and June and September 1997. Measurements were made with an Optronic Laboratories OL 754-O-PMT spectrophotometer equipped with a fiber-optic cable and an underwater sensor. Fluxes greater than the instrument's noise equivalent irradiance (NEI) level of 1×10^{-5} Wm^{-2} nm^{-1} just below the sea surface were measured at wavelengths of $\geq$294 nm. At 310 nm, the diffuse attenuation coefficient (K_d) ranged between 0.7 and 4.5 m^{-1}, with corresponding 10% depth penetrations between 4 and 0.5 m. This represents close to half of the summer mixed-layer water column in the Gulf of St. Lawrence. The following correlation coefficients were found: 0.81 between dissolved organic carbon (DOC) and K_d, 0.73 between chlorophyll *a* (Chl *a*) and K_d, and 0.73 between Chl *a* and DOC. The spectral variation of K_d suggests that yellow substance, and therefore DOC, is responsible for UV attenuation in these bodies of water.

Recent ozone losses and concurrent increases in ultraviolet-B (UVB, 280–320 nm) radiation, 7% in summer and 35% in winter (1989–1993), have been reported in temperate latitude regions (Kerr and McElroy 1993). A growing number of studies indicate that UVB radiation is harmful to aquatic organisms; reductions in productivity have been reported for phytoplankton and zooplankton, key levels of marine food chains (Cullen and Neale 1994; Williamson et al. 1994; Herndl 1997).

The penetration of UV radiation on freshwater ecosystems in midlatitude regions has recently been investigated (Kirk et al. 1994; Scully and Lean 1994; Morris et al. 1995; Laurion et al. 1997; Sommaruga and Psenner 1997). However, far fewer studies have evaluated the levels and impacts of UVB radiation on marine ecosystems at these latitudes (although *see* Piazena and Häder 1994), and there have been no evaluations of the estuary and Gulf of St. Lawrence. In these waters, productivity-determining biophysical interactions occur in a shallow mixed layer (10–15 m) (Therriault 1991; Runge and de Lafontaine 1996), where the eggs and larvae of several commercially important marine invertebrates and fishes are found (Fortier et al. 1992; Runge and de Lafontaine 1996). Experiments on two species found in the region, Atlantic cod (*Gadus morhua*) and the planktonic copepod *Calanus finmarchicus* (Kouwenberg et al. 1999*a,b*) found that egg mortality was strongly affected by exposure to UVB radiation.

An important aspect for studying potential effects of UVB irradiance on any aquatic ecosystem is the accurate measurement of underwater spectral irradiance. Oceanic ultraviolet irradiance measurements are often made with instruments that have a full-width half-maximum (FWHM) bandwidth of 10 nm and that are unable to measure fluxes at wavelengths <305 nm (Morris and Hargreaves 1997; Sommaruga and Psenner 1997). High-resolution UV measurements are essential for the application of biological weighting functions, especially for the shortest and most damaging wavelengths: 280–312 nm (Madronich 1993).

The overall objective of our research program is to determine whether ambient levels of UVB radiation and those predicted to occur as a result of ozone layer depletion (Wardle et al. 1997) are negatively affecting marine organisms in the estuary and Gulf of St. Lawrence. An essential first step in this effort is the measurement of ambient levels of UV radiation in the region. This paper presents: (1) high-resolution (1 nm) UV irradiance (290–400 nm) spectra for waters in the estuary and Gulf of St. Lawrence, (2) the associated diffuse attenuation coefficients ($K_{d\lambda}$) and 10% depth penetrations (depth to which 10% of the below-surface irradiance penetrates at any given wavelength), and (3) how DOC and Chl *a* concentrations are related to $K_{d\lambda}$.

Spectral downwelling irradiance was collected through the aperture of a submersible 100-mm-diameter integrating sphere attached to a scanning spectrophotometer (OL 754-O-PMT, Optronic Laboratories), via a 16-m UV-grade quartz fiber-optic cable. All parts of the integrating sphere, except the aperture, were shielded from the external light field. The integrating sphere (underwater sensor) was constructed to withstand depths of 20 m. The 25-mm aperture of the integrating sphere is covered with a hemispheric UV-grade acrylic dome (60% transmission at 300 nm), the cosine response of which has been tested underwater by Optronic Laboratories. The spectrophotometer is a double-monochromater design using 1,200 liter mm^{-1} aberration-corrected holographic gratings, optimized in the UVB. The wavelength resolution is given as 0.05 nm, with an accuracy in the UV of ±0.1 nm. The detector is a temperature-controlled S-20 photomultiplier (Hamamatsu). Optronic Laboratories specifies the stray light rejection to be 10^{-4} Wm^{-2} nm^{-1} and a spectroradiometric accuracy relative to the U.S. National Institute of Standards (NIST) of ±1–3%. This gives an absolute spectroradiometric accuracy in the UVB of approximately ±4.5%. The FWHM was set to 1 nm.

Before each field season, the instrument was calibrated at Optronic Laboratories. Prior to each cruise, it was calibrated against an NIST-traceable 200-W tungsten-halogen standard lamp (OL 752-10). The wavelength and gain accuracy were checked using an OL 752-159 dual calibration and gain check source module (wavelength accuracy of 0.1 nm) immediately before each set of measurements.

Measurements were made at 12 locations in the surface waters of the estuary and Gulf of St. Lawrence (Fig. 1; Table 1) from the research vessel the C.S.S. *Parizeau* in September 1996 and June 1997 and the N.G.C.C. *Martha L. Black* in September 1997. The underwater sensor was deployed ap-
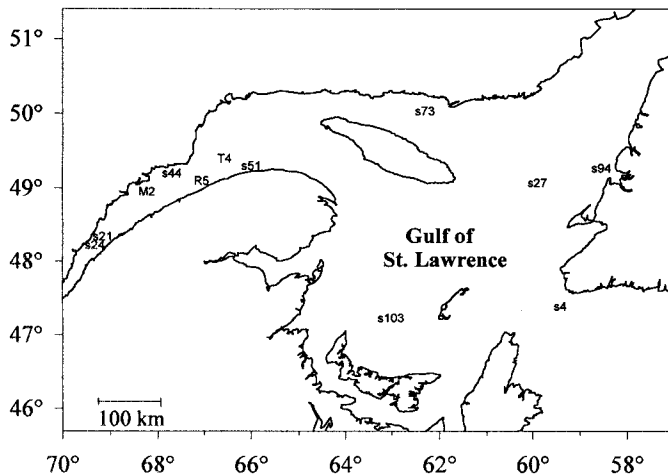
Fig. 1. Map of the estuary and Gulf of St. Lawrence, Canada, showing the location of stations at which high-resolution UV (290–400 nm) measurements were made in the surface waters for three separate cruises: September 1996 and June and September 1997. (Exact latitude and longitude are provided in Table 1.)

following the methods outlined by Mueller and Austin (1995). The integrating sphere was fixed in the center of an opaque black high-density polyethylene basin (1.2 m in diameter), 0.75 m away from a 1,000-W, current-stabilized quartz incandescent lamp. Using the OL 754 and the integrating sphere, irradiances were measured at 1-nm intervals between 280 and 800 nm in the air and under four water depths (as measured from the dome apex): 0.01, 0.03, 0.06, and 0.11 m; the seawater used was passed through a 40-μm filter. ICFs were calculated at 10-nm intervals between 280 and 400 nm and at 100-nm intervals up to 800 nm. Intermediate wavelengths were linearly interpolated. The values ranged between 1.6 and 1.8, similar to ICFs for other underwater radiometers (Satlantic 1997).

Underwater field measurements were corrected for ship shadow. Only the diffuse component of the global irradiance was affected by the ship shadow because the sun was kept within approximately ±45° of the beam of the ship during measurements. The spectral diffuse component of the global irradiance was measured on the deck of the vessel during the 1997 cruises using a shading disk technique immediately after depth profiles were completed. During the 1996 cruise, diffuse measurements were unavailable, so the diffuse UV irradiances were calculated using a delta-Eddington (Wiscombe 1977) radiative transfer model. This model has a 50-level, 100-km, plane-parallel atmosphere that accounts for the major UV attenuants (excluding cloud): Rayleigh scattering, aerosol extinction, and ozone absorption. Its inputs include station latitude, longitude, date, time of day, air surface temperature and pressure, and daily total ozone (measured at the Maurice Lamontagne Institute, Mont-Joli, Québec, 48°0.38′N, 68°0.09′W, with a Brewer MKIII double-monochrometer spectrophotometer [Sci-Tec Instruments]). A complete description of the radiative transfer model is provided by Davies et al. (1999). Ship shadow was determined by measuring irradiance at the side of the ship just above the water level and on the ship deck in the most obstruction-free area; corresponding reductions of diffuse irradiance were 30% for the *Parizeau* and 37% for the *Martha L. Black* and are spectrally neutral. Measured values were

proximately 2 m from the research vessel at midship. Vertical profiles consisted of measurements made at four depths, beginning just below the surface (depths of up to 1 m depending on the surface swell) and at 1-m intervals down to 3 m. At each depth, a 290–400-nm spectral scan was conducted at 1-nm intervals. Approximately 8 min were required for each scan. Measurements were made as close to solar noon as possible to reduce the changes in solar irradiance associated with changing solar elevation. Sky conditions were stable for all sets of measurements except those made at Sta. R5 and 94. At these two stations, the measurements were timed in an attempt to minimize surface irradiance differences caused by variable cloud conditions.

Because of the difference in indices of refraction between air (where the instrument is calibrated) and water (where it is operated), a correction factor must be applied to obtain in-water irradiances. The immersion correction factors (ICFs) applied to the data were determined experimentally

Table 1. Station location, date of measurement, and solar zenith angle at time of measurement, UV (290–400 nm) averaged attenuation coefficient correction factors $D_{o\,\overline{UV}}$ (Eq. 2, after Gordon 1989), the percent difference between corrected and uncorrected attenuation coefficients, *b* values (from Eq. 3), and DOC and Chl *a* values for the 1997 cruises.

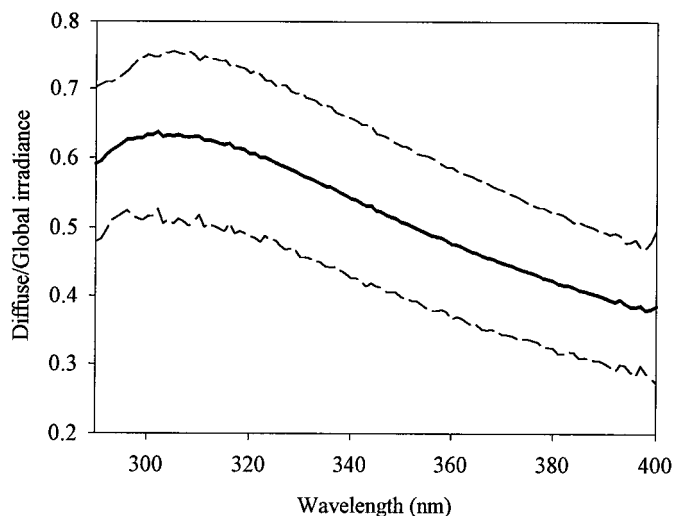| Station	Date	Latitude (W)	Longitude (N)	SZA (°)	$D_{o\,\overline{UV}}$	$[(K_{d\overline{UV}} - K_{d\overline{UV}}/D_o)/K_{d\overline{UV}}] \times 100\%$	*b* values (Eq. 3)	DOC (g m^{-3})	Chl *a* (μg liter^{-1})
M2	16 Sep 96	48° 55.65	68° 22.40	45.8	1.189	16	0.013	—	—
R5	17 Sep 96	49° 05.35	67° 05.83	46.7	1.193	16	0.010	—	—
T4	18 Sep 96	49° 49.00	66° 79.08	50.1	1.204	17	0.019	—	—
4	12 Jun 97	47° 38.95	59° 41.95	24.2	1.116	10	0.019	0.592	0.11
27	15 Jun 97	49° 07.25	59° 50.53	26.5	1.099	9	0.022	0.448	0.05
44	30 Aug 97	49° 00.18	67° 38.75	Overcast	1.197	16	0.013	1.818	2.02
21	1 Sep 97	48° 13.91	69° 26.58	40.1	1.177	15	0.015	3.589	1.265
24	1 Sep 97	48° 10.39	69° 22.89	54.1	1.293	23	0.015	2.564	0.88
51	2 Sep 97	49° 14.42	66° 10.27	Overcast	1.197	16	0.016	1.906	1.71
73	5 Sep 97	50° 03.45	62° 29.98	43.4	1.180	15	0.014	1.769	0.735
94	7 Sep 97	49° 27.04	50° 45.18	48.3	1.188	16	0.014	1.634	0.45
103	9 Sep 97	47° 22.96	63° 02.24	Overcast	1.197	16	0.018	1.806	1.365

Fig. 2. Spectral variation of the diffuse to global ratio averaged over all stations (excluding those with overcast conditions). Dashed lines show ±1 SD. On average, at wavelengths below 320 nm, the diffuse component dominates.

verified against calculations of the fraction of the sky obscured by the ships. Irradiance measurements were corrected by adding back in the obscured diffuse component of the light field. These corrections are significant, particularly in the UVB region of the spectrum, where the diffuse component can be dominant. For instance, below approximately 320 nm, an average of 60% of the incoming irradiance is diffuse (Fig. 2), which translates into ship shadow corrections of 18 and 22% for the *Parizeau* and *Martha L. Black,* respectively.

Diffuse attenuation coefficients ($K_{d\lambda}$) were calculated from

$$K_{d\lambda} = \frac{\ln\left(\dfrac{E_{-0\lambda}}{E_{z\lambda}}\right)}{\Delta z} \qquad (1)$$

where $E_{-0\lambda}$ and $E_{z\lambda}$ are irradiances measured just below the surface and at depth z (meters). Values of $K_{d\lambda}$ are considered to be quasi-inherent optical properties and are a commonly used descriptor of waterbodies (Kirk 1994; Booth and Morrow 1997). However, as the solar zenith angle (SZA) increases, the quasi-inherent nature of $K_{d\lambda}$ breaks down (Kirk 1984; Smith et al. 1991). For this set of measurements, the SZAs ranged from 24 to 54°; therefore, the attenuation coefficients were corrected for the geometric condition of the light field by dividing by Gordon's (1989) correction factor ($D_{o\lambda}$):

$$D_{o\lambda} = \frac{f_\lambda}{\cos \nu_{ow_\lambda}} + 1.197(1 - f_\lambda) \qquad (2)$$

where f_λ is the direct fraction of global irradiance (measured or calculated as above) and ν_{ow_λ} is the SZA below the water surface; this was determined by applying Snell's law to the SZA above the water surface, which was calculated following Michalsky (1988). Although $D_{o\lambda}$ varies with wavelength, averages over the UV band (D_{oUV}) were calculated for the

purpose of comparing corrected and uncorrected $K_{d\overline{UV}}$. $D_{o\overline{UV}}$ varied between 1.099 and 1.293, resulting in differences between uncorrected and corrected $K_{d\overline{UV}}$ of 9–23% (Table 1). Uncorrected values exceed corrected ones.

Surface waves cause fluctuations in irradiances measured underwater, and corresponding extinction coefficients, about an average value (Smith and Baker 1984). To eliminate the noise, $K_{d\lambda}$ values calculated for each station were fitted, using the least squares method, to a two-parameter exponential decay formula

$$K_{d\lambda} = a e^{-b\lambda} \qquad (3)$$

and extrapolated to 290 nm. The average b value was 0.0157 ± 0.0034 (all values are listed in Table 1), which is similar to values previously reported for yellow substance absorption (Bricaud et al. 1981; Carder et al. 1989), suggesting that gelbstoff is responsible for the attenuation of the wavelengths measured. Examples of the measured and fit values of $K_{d\lambda}$ are shown for the most poorly fit station (94), a day with swells of 1.5 m, and Sta. 24, a calm day (Fig. 3). For all stations, the adjusted r^2 values of the best-fit curves ranged from 0.67 to 0.99; over 70% exceeded 0.90. The 10% depth penetrations ($z_{\lambda10\%}$) were calculated by

$$z_{\lambda10\%} = \frac{0.230}{K_{d\lambda}} \cdot \frac{1}{\overline{D_{o\lambda}}} \qquad (4)$$

where $\overline{D_{o\lambda}}$ (1.19) is the average value for the study region.

Water samples for DOC and Chl *a* analysis were taken from a depth of 5 m during the 1997 field season (Table 1). Subsamples of 250 ml were filtered on Whatman GF/F filters and extracted with 90% acetone for 24 h at 4°C for the determination of Chl *a* using the fluorometric method of Yentsch and Menzel (1963), as modified by Hölm-Hansen et al. (1965) and Welschmeyer (1992). Samples for DOC analysis during the June 1997 cruise were collected in 250-ml fluorinated polyethylene bottles (Nalgene) that had been soaked overnight in 10% HCl (w/v), rinsed five times in distilled water, and oven dried at 80°C. Samples were frozen immediately and analyzed by high-temperature catalytic oxidation in an Ionics model 1500 carbon analyzer (Kepkay et al. 1997). Samples for DOC analysis during the September 1997 cruise were collected in 50-ml glass vials with Teflon septa. The vials had been rinsed in distilled water, soaked for 24 h in 10% HCl, wrapped in aluminum foil, and combusted at 500°C for 24 h. The Teflon lids underwent the same rinsing procedure, were oven dried at 90°C for 24 h, and then were wrapped in precombusted foil. Water samples were filtered with precombusted Whatman GF/F filters, acidified to pH 1.0, and frozen until analysis in a Shimadzu TOC-5000 high-temperature oxidation instrument (Sharp et al. 1993).

The highest UV levels were measured at Sta. 27 on 12 June 1997, a sunny day (Fig. 4A). Measurements from Sta. 103, 9 September 1997, an overcast day, are shown in Fig. 4B for comparison. Station-averaged spectral fluxes (made just below the surface) and corresponding standard deviations indicate variability up to two orders of magnitude (Fig. 4C). Variability is caused by changes in solar elevation, sea surface conditions, and water and atmospheric constituents. The average flux at 300 nm is 1.1×10^{-3} Wm^{-2} nm^{-1}.
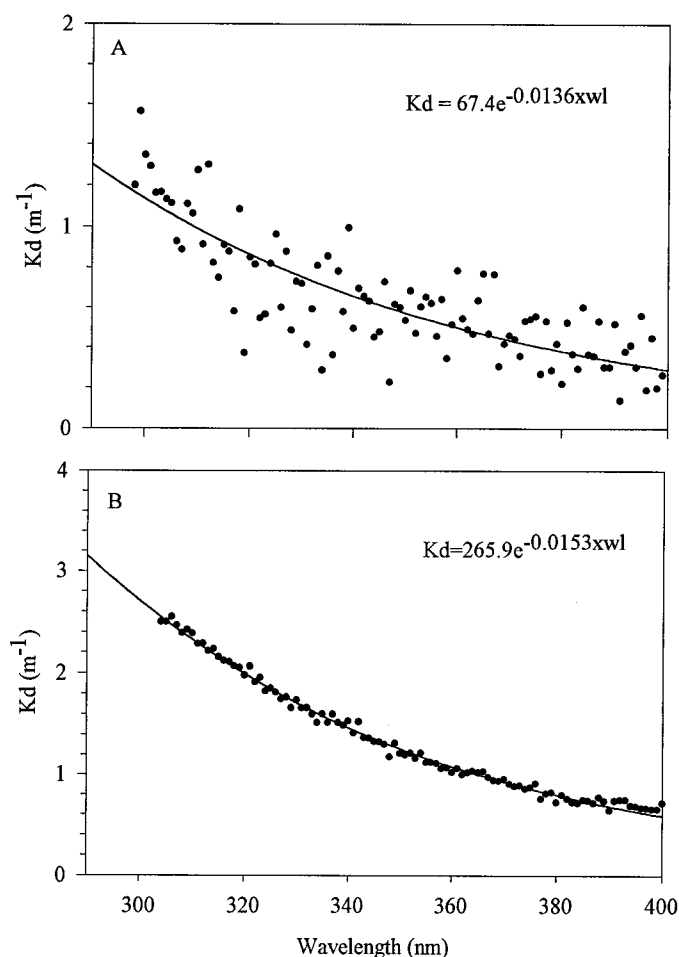
Fig. 3. Diffuse attenuation coefficients (K_d) measured at (A) Sta. 94, and (B) Sta. 24. Values were fit with a two-parameter exponential decay formula (*see Eq. 3 in the text*) to mitigate fluctuations about an average value caused by surface waves. Surface swells of 1.5 m were observed at Sta. 94, while conditions at Sta. 24 were calm.
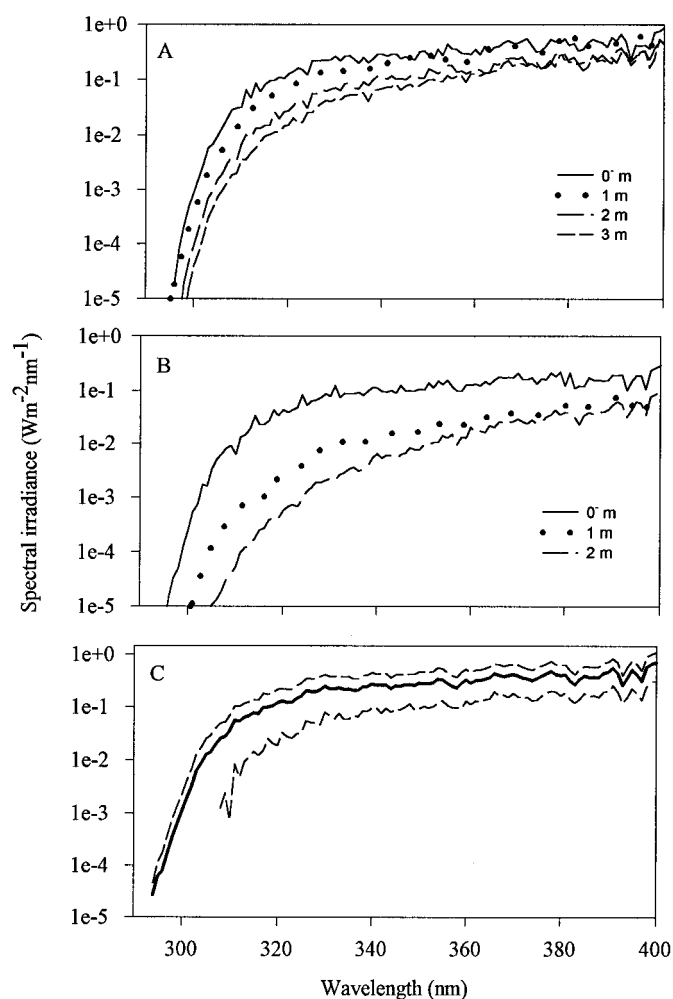

Fig. 4. Irradiance vs. wavelength at different depths measured at (A) Sta. 27 on 15 June 1997 under clear-sky conditions, and (B) Sta. 103 on 9 September 1997 under overcast conditions. Station-averaged spectral fluxes (C), made just below the surface, and corresponding standard deviations.

Detectable fluxes (greater than the instrument's NEI of 1×10^{-5} Wm^{-2} nm^{-1}) just below the surface were measured at wavelengths as low as 294 nm (Sta. T4). There was little variation in this lower wavelength limit among stations: 296 ± 2 nm.

At 300 nm, K_d values range from approximately 1 to 5 m^{-1}, with corresponding 10% depths of 2.3 and 0.4 m. At 400 nm, K_d values vary between 0.2 and 1.4 m^{-1}, and the 10% depths are 21 and 1.4 m (Fig. 5). The 10% depths are generally smallest in the estuary and become greater toward the Gulf (10% depths at 310 nm are shown in Fig. 6). All values fall within the range of 10% depths presented in the review article by Booth and Morrow (1997): at 310 nm, a depth of 0.1 m was recorded by Scully and Lean (1994) in Lake Cromwell, Québec, and values as high as 20 m were reported for the clearest ocean waters by Smith and Baker (1979) (Fig. 5).

The lowest DOC and Chl *a* values were measured at Sta. 27, and the highest values were recorded in the estuary at Sta. 21 and 44, respectively (Table 1). The DOC values for the estuary and Gulf are similar to those reported for the same regions by Sharp et al. (1982), Pocklington (1985), and Packard et al. (unpubl. data). Similarly, the Chl *a* measurements listed in Table 1 are comparable to values previously recorded in this region during the same months (Savenkoff pers. comm.).

Spearman's correlations were used to examine the relationship between attenuation coefficients and concentrations of Chl *a* and DOC. Correlations were determined for K_d at 10-nm intervals, between 290 and 400 nm, using the estimated values. For all wavelengths, DOC was more highly correlated with K_d than Chl *a*. The average correlation coefficient between DOC and K_d was 0.81; between Chl *a* and K_d, 0.73; and between Chl *a* and DOC, 0.73. In other marine environments, Chl *a* is highly correlated with UV attenuation (Stambler et al. 1997). In freshwater, DOC (often several orders of magnitude higher than the values reported here) is the dominant factor in UV attenuation, and Chl *a* is unimportant (Scully and Lean 1994; Morris et al. 1995; Laurion et al.
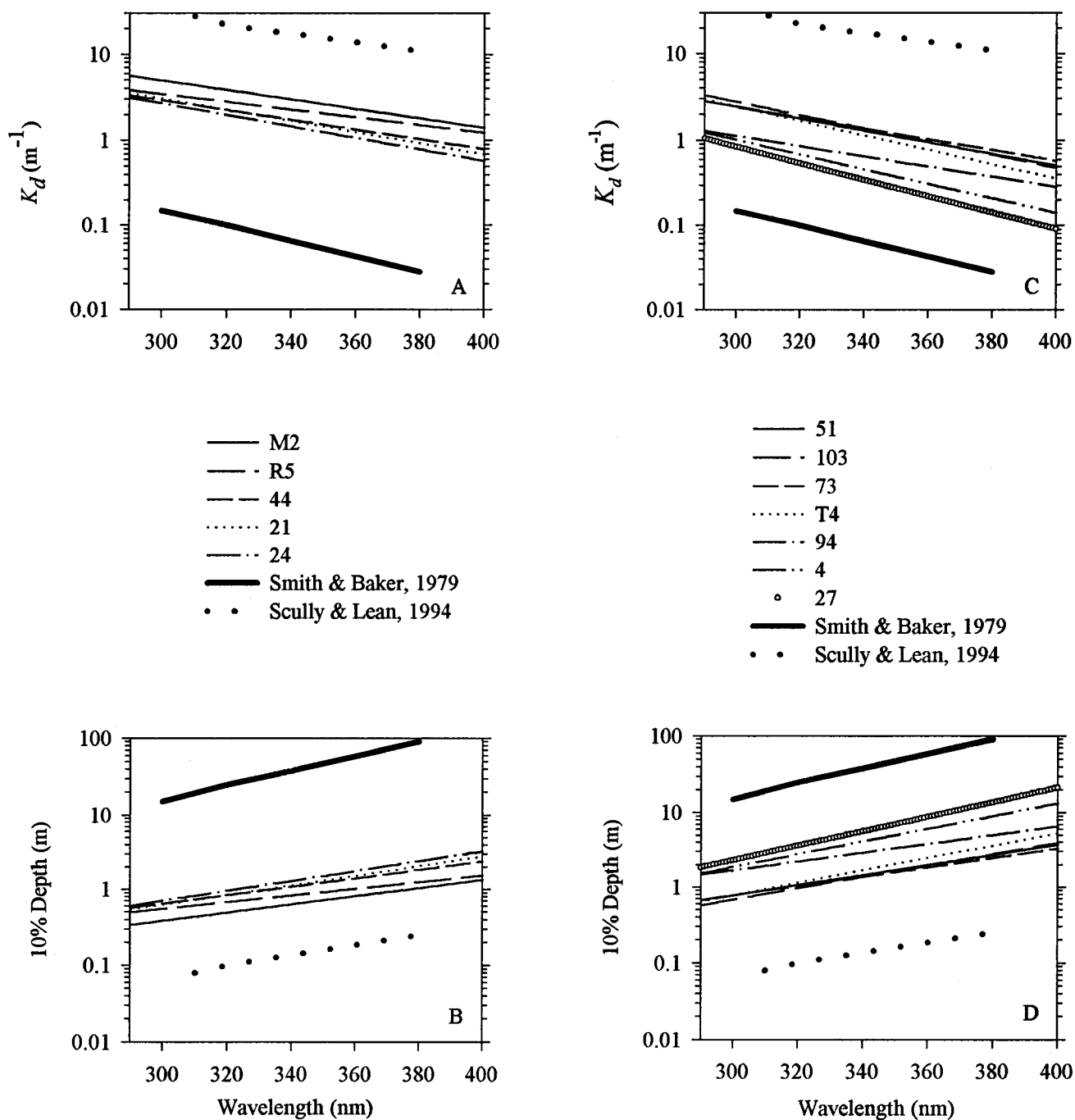
Fig. 5.   Diffuse attenuation coefficients and associated 10% depths (depth to which 10% of irradiance just below the surface penetrates) of estuary stations (A and B) and Gulf stations (C and D). All values fall within the range of values reported by Scully and Lean (1994) in Lake Cromwell, Québec, and Smith and Baker (1979) for the clearest ocean waters.

1997). The significant autocorrelation between DOC and Chl *a* in this data set makes it difficult to determine their respective contributions to the diffuse attenuation coefficients; however, the *b* values imply that yellow substance, and therefore DOC, is important. A significantly larger data set, including stations where Chl *a* and DOC concentrations varied inversely, would be needed to determine the relative contributions to UV radiation attenuation in these bodies of water.

The 10% depths, under ambient conditions, penetrate a substantial portion (up to 50%) of the summer mixed-layer water column. Therefore, the early life stages of the crustacean and fish species present in this shallow layer may be affected by UV radiation. Combining the following four components into a simulation model will allow a more rigorous quantitative assessment of UV effects on marine species in the estuary and Gulf of St. Lawrence: (1) irradiance
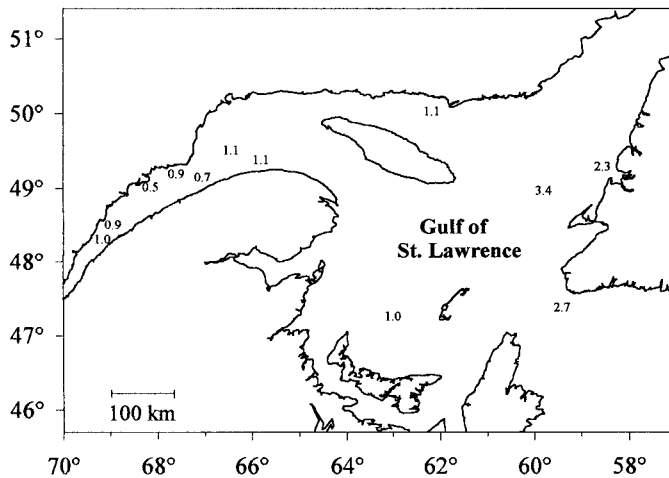
Fig. 6. The 10% depths (calculated using estimated values of K_d) at 310 nm for all stations. Station numbers are presented in Fig. 1.

measurements such as those reported here, (2) high spectral resolution biological weighting functions for UVB-induced mortality of specific species (e.g., Kouwenberg et al. 1999*a,b*), (3) data on the vertical distribution of the target species and their various life stages in the mixed layer of the water column (with a greater resolution in the upper 10 m than currently exists), and (4) development of a model to predict the vertical position of passive particles (such as eggs) in the mixed layer (e.g., Neale et al. 1998). The high-resolution measurements presented here represent an important first step toward building such a model.

Penny Kuhn[1]

CONFORTE (Consulting For The Environment)
Dundas, Ontario, Canada L9H 3W3

Howard Browman[2]

Maurice Lamontagne Institute
Fisheries and Oceans Canada, Science Branch
Laurentian Region, Division of Ocean Sciences
Mont-Joli, Québec, Canada G5H 3Z4

---

[1] Present address: Department of Oceanography, Dalhousie University, Halifax, Nova Scotia, Canada B3H 4J1.

[2] Present address: Institute of Marine Research, Aquaculture Centre, Austevoll Aquaculture Research Station, N-5392 Storebø, Norway.

Bruce McArthur

Atmospheric Environment Service
Environment Canada
Downsview, Ontario, Canada M3H 5T4

Jean-Francois St-Pierre

Maurice Lamontagne Institute
Fisheries and Oceans Canada, Science Branch
Laurentian Region, Division of Ocean Sciences
Mont-Joli, Québec, Canada G5H 3Z4

References

BOOTH, C. R., AND J. H. MORROW. 1997. The penetration of UV into natural waters. Photochem. Photobiol. **65:** 254–257.

BRICAUD, A., A. MOREL, AND L. PRIEUR. 1981. Absorption of dissolved organic matter of the sea (yellow substance) in the UV and visible domains. Limnol. Oceanogr. **26:** 43–53.

CARDER, K. L., R. G. STEWARD, G. R. HARVEY, AND P. B. ORTNER. 1989. Marine humic and fulvic acids: Their effects on remote sensing of ocean chlorophyll. Limnol. Oceanogr. **34:** 68–81.

CULLEN, J. J., AND P. J. NEALE. 1994. Ultraviolet radiation, ozone depletion, and marine photosynthesis. Photosynth. Res. **39:** 303–320.

DAVIES, J. A., P. S. KUHN, G. DUHAMMEL, AND K. RUNNALLS. 1999. An ultraviolet (290–325 nm) irradiation model for Canada. Phys. Geogr. In press.

FORTIER, L., M. E. LEVASSEUR, R. DROLET, AND J-C. THERRIAULT. 1992. Export production and the distribution of fish larvae and their prey in a coastal jet frontal system. Mar. Ecol. Prog. Ser. **85:** 203–218.

GORDON, H. 1989. Can the Lambert–Beer law be applied to the diffuse attenuation coefficient of ocean water? Limnol. Oceanogr. **34:** 1389–1409.

HERNDL, G. J. 1997. Role of ultraviolet radiation on bacterioplankton activity, p. 143–150. *In* D-P. Häder [ed.], The effects of ozone depletion on aquatic ecosystems. Landes.

HÖLM-HANSEN, O., C. J. LORENZEN, R. N HOLMES, AND J. S. STRICKLAND. 1965. Fluorometric determination of chlorophyll. J. Cons. Int. Explor. Mer **30:** 3–15.

KEPKAY, P. E., S. E. H. NIVEN, AND J. F. JELLETT. 1997. Colloidal organic carbon and phytoplankton speciation during a coastal bloom. J. Plankton Res. **19:** 369–389.

KERR, J. B., AND C. T. MCELROY. 1993. Evidence for large upward trends of ultraviolet-b radiation linked to ozone depletion. Science **262:** 1032–1034.

KIRK, J. T. O. 1984. Dependence of relationship between inherent and apparent optical properties of water on solar altitude. Limnol. Oceanogr. **29:** 350–356.

———. 1994. Optics of UV-B radiation in natural waters. Arch. Hydrobiol. **43:** 1–16.

———, AND OTHERS. 1994. Measurements of UV-B radiation in two freshwater lakes: An instrument intercomparison. Arch. Hydrobiol. **43:** 71–99.

KOUWENBERG, J. H. M., H. I. BROWMAN, J. J. CULLEN, R. F. DAVIS, J-F. ST-PIERRE, AND J. A. RUNGE. 1999*a*. Biological weighting of ultraviolet (280–400 nm) induced mortality in marine zooplankton and fish. I. Atlantic cod (*Gadus morhua*) eggs. Mar. Biol. In press.

———, ———, J. A. RUNGE, J. J. CULLEN, R. F. DAVIS, AND J-F. ST-PIERRE. 1999*b*. Biological weighting of ultraviolet (280–400 nm) induced mortality in marine zooplankton and fish. II. (*Calanus finmarchicus*) eggs. Mar. Biol. In press.

LAURION, I., W. F. VINCENT, AND D. R. S. LEAN. 1997. Underwater

ultraviolet radiation: Development of spectral models for northern high latitude lakes. Photochem. Photobiol. **65:** 107–114.

MADRONICH, S. 1993. UV radiation in the natural and perturbed atmosphere, p. 17–69. *In* M. Tevini [ed.], UV-B radiation and ozone depletion. Lewis.

MICHALSKY, J. L. 1988. The Astronomical Almanac's algorithm for approximate solar position (1950–2050). Sol. Energy **40:** 227–235.

MORRIS, D. P., AND B. R. HARGREAVES. 1997. The role of photochemical degradation of dissolved organic carbon in regulating the UV transparency of three lakes on Pocono Plateau. Limnol. Oceanogr. **42:** 239–249.

———, AND OTHERS. 1995. The attenuation of solar UV radiation in lakes and the role of dissolved organic carbon. Limnol. Oceanogr. **40:** 1381–1391.

MUELLER, J. L., AND R. W. AUSTIN. 1995. Ocean optics protocols for SeaWiFS validation. v. 25. SeaWiFS Technical Report Ser. **24–25.**

NEALE, P. J., R. F. DAVIS, AND J. J. CULLEN. 1998. Interactive effects of ozone depletion and vertical mixing on photosynthesis of Antarctic phytoplankton. Nature **392:** 585–589.

PIAZENA, H., AND D. P. HÄDER. 1994. Penetrations of solar UV irradiation in coastal lagoons of the southern Baltic Sea and its effect on phytoplankton communities. Photochem. Photobiol. **60:** 463–469.

POCKLINGTON, R. 1985. Organic matter in the Gulf of St. Lawrence in winter. Can. J. Fish. Aquat. Sci. **42:** 1556–1561.

RUNGE, J. A., AND Y. DE LAFONTAINE. 1996. Characterization of the pelagic ecosystem in surface waters of the northern Gulf of St. Lawrence in early summer: The larval redfish–*Calanus*–microplankton interaction. Fish. Oceanogr. **5:** 21–37.

SATLANTIC. 1997. SeaWiFS profiling multichannel radiometer user's manual. SPMR 017.

SCULLY, N. M., AND D. S. LEAN. 1994. The attenuation of ultraviolet radiation in temperate lakes. Arch. Hydrobiol. **43:** 135–144.

SHARP, J. H., R. BENNER, L. BENNETT, C. A. CARLSON, R. DOW, AND S. E. FITZWATER. 1993. Re-evaluation of high temperature combustion and chemical oxidation measurements of dissolved organic carbon in seawater. Limnol. Oceanogr. **38:** 1774–1782.

———, C. H. CULBERSON, AND T. M. CHURCH. 1982. The chemistry of the Delaware Estuary: General consideration. Limnol. Oceanogr. **27:** 1015–1028.

SMITH, R. C., AND K. S. BAKER. 1979. Penetration of UV-B and biologically effective dose-rates in natural waters. Photochem. Photobiol. **29:** 311–323.

———, AND ———. 1984. The analysis of ocean optical data, p. 119–126. SPIE. v. 489. Ocean Optics VII.

———, K. J. WATERS, AND K. S. BAKER. 1991. Optical variability and pigment biomass in the Sargasso Sea as determined using deep-sea optical mooring data. J. Geophys. Res. **96(C5):** 8665–8686.

SOMMARUGA, R., AND R. PSENNER. 1997. Ultraviolet radiation in a high mountain lake of the Austrian alps: Air and underwater measurements. Photochem. Photobiol. **65:** 957–963.

STAMBLER, N., C. LOVENGREEN, AND M. M. TILZER. 1997. The underwater light field in the Bellingshausen and Amundsen Seas (Antarctica). Hydrobiologia **344:** 41–56.

THERRIAULT, J-C. [ED.]. 1991. The Gulf of St. Lawrence: Small ocean or big estuary? Canada Special Publication of Fisheries and Aquatic Science **113.**

WARDLE, D. I., J. B. KERR, C. T. MCELROY, AND D. R. FRANCIS [EDS.]. 1997. Ozone science: A Canadian perspective on the changing ozone layer. Environment Canada.

WELSCHMEYER, N. A. 1992. Fluorometric analysis of chlorophyll *a* in the presence of chlorophyll *b* and phaeopigments. Limnol. Oceanogr. **39:** 1985–1992.

WILLIAMSON, C. E., H. E. ZAGARESE, P. C. SCHULZE, B. R. HARGREAVES, AND J. SEVA. 1994. The impact of short-term exposure to UV-B radiation on zooplankton communities in north temperate lakes. J. Plankton Res. **16:** 205–218.

WISCOMBE, W. J. 1977. The delta-Eddington approximation for a vertically inhomogeneous atmosphere. NCAR Technical Note—121+STR.

YENTSCH, C. S., AND D. W. MENZEL. 1963. A method for the determination of phytoplankton chlorophyll and phaeophytin by fluorescence. Deep-Sea Res. **10:** 221–231.

Bicarbonate addition promotes coral growth

Abstract—The addition of 2 mM bicarbonate to aquaria containing tropical ocean water and branches of *Porites porites* caused a doubling of the skeletal growth rate of the coral. Nitrate or ammonium addition (20 μM) to oligotrophic seawater caused a significant reduction in coral growth, but when seawater containing the extra bicarbonate was supplemented with combined nitrogen, no depression of the higher growth rate was evident. We infer that (1) the present dissolved inorganic carbon (DIC) content of the ocean limits coral growth, (2) this limitation is exacerbated by nitrate and ammonium, and (3) adding DIC increases coral calcification rates and confers protection against nutrient enrichment.

Dissolved inorganic carbon (DIC) is used by all hard corals for growth of $CaCO_3$ skeletons. Hermatypic corals (reef-building corals that harbor zooxanthellae) also require DIC for photosynthesis. Until recently, the general view has been that, at concentrations greater than 2 mM, DIC in seawater is in ample supply compared with other essential solutes such as nitrate and phosphate and trace elements such as iron, zinc, and silicon. There is, however, a growing awareness (Raven 1993) that the supply of DIC limits photosynthesis in planktonic algae, seagrasses (Beer and Rehnberg 1997), coccolithophores (Merrett et al. 1993; Israel and Gonzales 1996), and macroalgae (Johnston et al. 1992). Several authors (Muscatine et al. 1989*b*; Weis et al. 1989; Dubinsky et al. 1990; Lesser et al. 1994) have speculated on DIC limitation in coral. The only study that tested experimentally the effect of adding DIC (Burris et al. 1983) focused only on photosynthesis and was inconclusive.